Colloid Polym Sci (2004) 282: 602–612
DOI 10.1007/s00396-003-0985-z

ORIGINAL CONTRIBUTION

Stephen B. Johnson
David E. Dunstan
George V. Franks

A novel thermally-activated crosslinking agent for chitosan in aqueous solution: a rheological investigation

Received: 23 January 2003
Accepted: 12 August 2003
Published online: 10 October 2003

S. B. Johnson
Department of Geological and Environmental Sciences,
Stanford University, Building 320,
Stanford, CA 94305–2115, USA

D. E. Dunstan
Department of Chemical Engineering,
University of Melbourne,
Parkville, Victoria 3010, Australia

G. V. Franks (✉)
Department of Chemical Engineering,
University of Newcastle, Callaghan,
New South Wales 2308, Australia
E-mail: george.franks@newcastle.edu.au
Tel.: +61 2 4921-5889
Fax: +61 2 4921-6920

Abstract The use of 2,5-dimethoxy-2,5-dihydrofuran (DHF) as a temperature-controlled gelation agent for chitosan under acidic conditions has been examined by dynamic oscillatory and viscometry techniques. In particular, the rate and extent of gelation have been examined over a range of different temperatures (40–98 °C), DHF concentrations (10–100 mM) and pH conditions (0.9–2.1). The gelation time, t_G, decreases, and the maximum gelation rate increases substantially as a function of rising temperature. When fit with a simple Arrhenius function, the t_G data yield an activation energy for gelation of 55 ± 8 kJ mol^{-1}. Gelation is found to occur on the shortest time-scale, and the strongest gels result, at the highest DHF concentrations investigated. Similarly, the gelation rate and gel strength are highest for the most acidic solution conditions examined. Experimental findings are interpreted in terms of a competition between the crosslinking reaction (which drives gel formation, and is initially dominant) and protolytic decomposition of chitosan (which disrupts the gel structure, and becomes increasingly important as time progresses). Syneresis phenomena additionally impact results obtained at DHF concentrations ≥50 mM.

Introduction

After cellulose, chitin is the most abundant polysaccharide found in nature due to its presence in crustacean shells, insect exoskeletons and fungal biomass [1]. Structurally, it consists primarily of 1,4-linked units of 2-acetamido-2-deoxy-β-D-glucose and, except under highly acidic conditions, is insoluble in aqueous media. The solubility of chitin can be significantly enhanced through a process of deacylation, in which the *N*-acetyl linkage is hydrolyzed under very alkaline conditions to produce an amine moiety. The biopolymer chitosan results. In addition to being readily soluble in dilute acids, chitosan has been found to possess many useful properties. These include its low toxicity, biocompatibility, anti-microbial action, susceptibility to enzymatic degradation and strong affinity for many ionic species in solution [2, 3, 4]. As a result, chitosan possesses a wide range of potential applications. These include its use in metal and dye binding agents, food and cosmetic products, fiber and film forming agents, flocculants for waste effluents, biodegradable packaging materials, and biomedical products such as wound dressings, transfection agents, and pharmaceutical products [4, 5, 6, 7, 8, 9, 10, 11, 12, 13, 14, 15].

When solubilized in aqueous solution, chitosan can form weak intermolecular links through hydrophobic interactions between residual acetyl groups [16, 17, 18]. The formation of far stronger and more extensive intermolecular associations is possible through physical (ionotropic) or chemical (covalent bond forming) crosslinking processes, which impart additional

valuable properties to the resulting products. In particular, crosslinking can be used to enhance mechanical strength [19, 20, 21, 22, 23] and chemical stability [24], control aqueous permeability [23,25, 26, 27, 28, 29] and solubility [30, 31, 32], and decrease the aqueous swelling characteristics [21,22,24, 25, 26, 28, 33, 34] of chitosan-based materials. In addition, controlled crosslinking enables the size/thickness, shape, surface morphology and hardness of chitosan objects to be manipulated [27, 28, 29, 31, 35, 36, 37, 38]. As a result, crosslinked chitosan products have been widely investigated for use in a broad range of applications in which inexpensive, geometrically and morphologically well-defined, chemically and physically robust, solid objects possessing a high level of biocompatibility and/or low toxicity are desired. Examples include the use of crosslinked chitosan materials as controlled-release drug delivery supports (e.g. [23,26, 27, 28, 29, 30, 31, 34, 35, 36, 37, 38, 39, 40, 41, 42, 43, 44, 45, 46, 47, 48, 49, 50, 51, 52, 53]), biomedical scaffolds (e.g. [54, 55]), biochemical separation membranes (e.g. [25, 56, 57]), catalyst supports (e.g. [58]) and enhanced metal ion and dye recovery agents (e.g. [32, 59, 60, 61, 62, 63, 64, 65, 66, 67, 68, 69, 70, 71]).

When undertaken in an aqueous medium, control of chitosan crosslinking can be complicated due to the rapid rate of reaction between the biopolymer functional groups (typically the amine moieties) and many crosslinking agents. In particular, several previous studies have demonstrated that chemical gelation reactions between chitosan and simple dialdehyde crosslinkers such as glutaraldehyde progress very rapidly in aqueous media. For example, Hsien and Rorrer [61] have reported that under their concentrated experimental conditions, the homogeneous crosslinking reaction between chitosan and glutaraldehyde results in formation of a rigid gel within 1 min at 27 °C. Similarly, Mi et al. [33] have recently shown that for a moderately concentrated solution (1 wt%) of a high molecular weight chitosan (MW = 2 000 000) at 30 °C, aqueous-based gelation takes place in less than 12 min over the range of much lower glutaraldehyde concentrations examined. Thanoo et al. [28] have further reported that the 'instantaneous' aqueous-based reaction of chitosan with glutaraldehyde leads to a loss of control over the geometry and surface morphology of chitosan microspheres. In order to slow such crosslinking reactions sufficiently to allow controlled, homogeneous crosslinking to occur, many studies (e.g. [28, 29, 35, 36, 42, 43, 49]) have utilized chemical crosslinking agents such as glutaraldehyde solubilized in alternative toxic non-aqueous phases.

In this study, we present an alternative method for slowing and controlling the chemical gelation of chitosan in aqueous solution based on the use of a thermally-activated crosslinking agent, butenedial. Both the onset time and rate of the gelation process have been manipulated by controlling the butenedial concentration through the use of a precursor molecule, 2,5-dimethoxy-2,5-dihydrofuran (DHF). When exposed to an acidic aqueous environment, Hansen et al. [72] have shown that DHF will gradually protolytically decompose to form butenedial. They also demonstrated that the decomposition rate is extremely sensitive to the solution temperature, being ca. 80–90% complete within 2 h at temperatures in excess of 95 °C, but slowing markedly at lower temperatures. As a result, manipulation of the solution temperature should give access to a wide range of different gelation rates and times in acidic chitosan–DHF mixtures. Regulation of the solution pH and DHF concentration is expected to allow further control over the characteristics of the crosslinking reaction [73].

For the purposes of this study, the gelation of chitosan using DHF in acidic aqueous media has been investigated using two macroscopic rheological methods, namely small amplitude dynamic oscillatory and viscosity techniques. The effects of temperature, DHF concentration and pH have been examined in detail. Unfavourable protolytic decomposition and syneresis processes have also been considered. Where appropriate, data have been compared with findings from previous studies of aqueous chitosan systems. The results serve to demonstrate the potential usefulness of DHF as a controlled crosslinking agent for chitosan in aqueous systems.

Experimental section

Materials

A high molecular weight chitosan (MW≈2 000 000) with a degree of acylation of approximately 87% [47] was obtained from Fluka Biochimika (Switzerland). Analytical grade hydrochloric acid and cis/trans 2,5-dimethoxy-2,5-dihydrofuran (DHF) were purchased from Ajax Chemicals (Australia) and Tokyo Kasei (Japan) respectively. Milli-Q grade water (conductivity $\approx 10^{-6}$ S m^{-1} at 20 °C) was used in all experiments.

Chitosan solutions were prepared by slowly dissolving a known mass (1.5 wt%) of the biopolymer in suitable concentrations (0.06–0.2 M) of aqueous HCl. They were used within 12 h of preparation in order to minimize the possibility of chitosan degradation. A micro-syringe was used to transfer DHF directly into the acidified chitosan solutions. The resulting mixtures were vigorously shaken, followed by slow end-over-end tumbling for several minutes. They were then allowed to stand briefly before measurement in order to eliminate air bubbles from solution.

Methods

Small amplitude dynamic oscillatory measurements were undertaken in a cone-and-plate geometry using the 'oscillation strain control' and 'oscillation stress sweep' functions of a Stresstech Rheometer (RheoLogica Instruments, Sweden) in combination

with a 30 mm, 4° cone and an elevated temperature cell (CCE). Evaporation was prevented by coating the chitosan solutions with a layer of silicone oil (viscosity = 2 000 centipoise) and sealing the sample-holding region with an insulated cover. All dynamic oscillatory experiments were performed using strains lying within the linear viscoelastic region of the chitosan samples. For time-based gelation measurements of aqueous chitosan–DHF systems, the applied strain was initially determined by the lower stress limit of the rheometer (strain≈0.01). As gelation proceeded, the use of lower strains became possible and, for gelled samples, a limiting strain of 0.001 was used. This small value ensured that the induced deformation did not adversely affect the measured rate or extent of gelation. For dynamic oscillatory measurements of chitosan solutions in the absence of DHF, significantly higher limiting strains (0.05–0.1) were required in order to adequately resolve the experimental signal from background noise. The latter strains were again found to lie well within the region of linear viscoelastic response. Frequency sweeps were performed in the range of 0.02 to 20 Hz, although the results presented in this paper were measured at 1 Hz.

Viscosity measurements were performed using the 'viscometry' function of the Stresstech Rheometer, again in a cone-and-plate geometry. Unfortunately, the use of silicone oil to prevent evaporation was not viable due to it mixing with the chitosan samples at moderate to high shear rates. Instead, a water bath was used to heat chitosan solution at the desired temperatures (40–95 °C) in sealed vessels. At selected time intervals, the samples were removed from the water bath, rapidly cooled, and their viscosity properties measured at a common temperature of 20 °C. Under the latter condition, evaporation was not found to significantly affect the solution viscosity over the time-scale of the measurement.

Analyses of the syneresis properties of several chitosan–DHF systems were undertaken by placing relevant chitosan–DHF samples in sealed glass vials, which were again heated using a water bath. At specified time intervals, samples were removed from the bath, the crosslinking reaction quenched by immersing the sealed vials in cold water, and the extent of syneresis immediately determined by measuring the mass of free water expelled from the bulk gel medium.

Results and discussion

Impact of temperature on chitosan–DHF gelation kinetics

The storage moduli (G') and phase lag (δ, where tan δ = G"/G') properties of an aqueous 1.5 wt% chitosan–25 mM DHF solution are shown as a function of time, t, and temperature in Figs. 1 and 2, respectively. The temperature range examined is 40–98 °C and the pH is 1.4 in all cases. G" data are not shown due to δ rapidly approaching zero as gelation proceeds. Under such circumstances, accurate measurements of δ were limited by the instrument resolution, with large proportional errors in δ being typically obtained as $\delta \rightarrow 0$. As a result, the calculated values of G" were generally found to be unreliable beyond the initial stages of gelation.

The data of Figs. 1 and 2 show a strong dependence on temperature. At the lowest temperatures investigated, the initial rate of gelation is extremely slow, with G' increasing very gradually and δ remaining relatively constant at 80 ± 5°. Such behaviour is consistent with the gradual formation of distinct, crosslinked chitosan aggregates in solution as a precursor to the formation of a continuous, three-dimensional crosslinked chitosan network [74]. For higher temperature systems, however, Fig. 1 shows that the initial rate of increase of G', $\Delta G'/\Delta t$, rises as a function of temperature, indicating a progressively more rapid transition to the formation of a ubiquitous three-dimensional crosslinked system. The data of Fig. 2 are consistent with these findings, showing that δ decreases most rapidly for the highest temperature chitosan–DHF systems. The impacts of temperature on

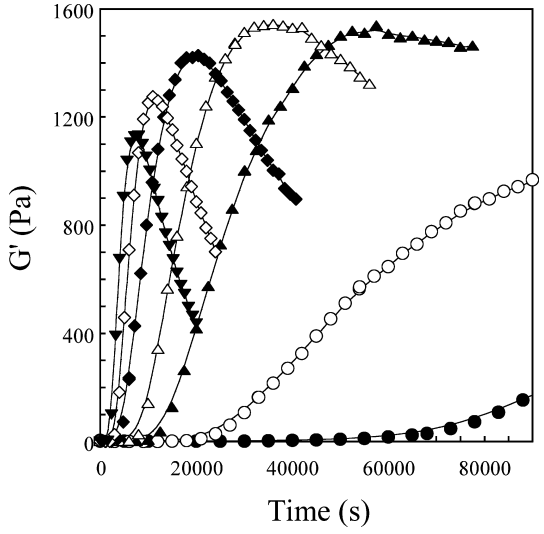

Fig. 1 The storage modulus of a 1.5 wt% chitosan–25 mM DHF solution at pH 1.4 as a function of temperature and time. ● 40 °C, ○ 50 °C, ▲ 60 °C, △ 70 °C, ◆ 80 °C, ◇ 90 °C, ▼ 98 °C

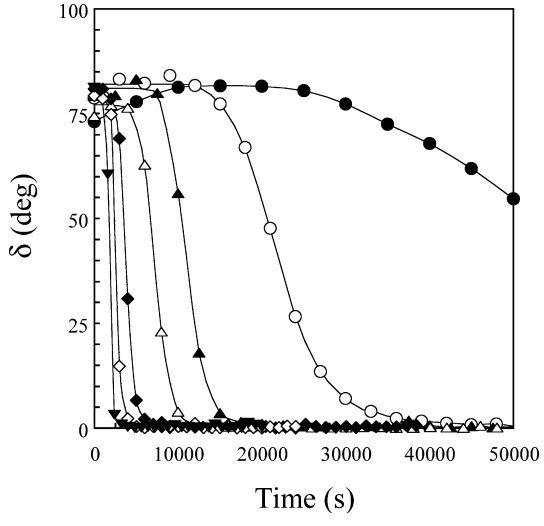

Fig. 2 The phase lag, δ, measured for a 1.5 wt% chitosan–25 mM DHF solution at pH 1.4 as a function of temperature and time. ● 40 °C, ○ 50 °C, ▲ 60 °C, △ 70 °C, ◆ 80 °C, ◇ 90 °C, ▼ 98 °C

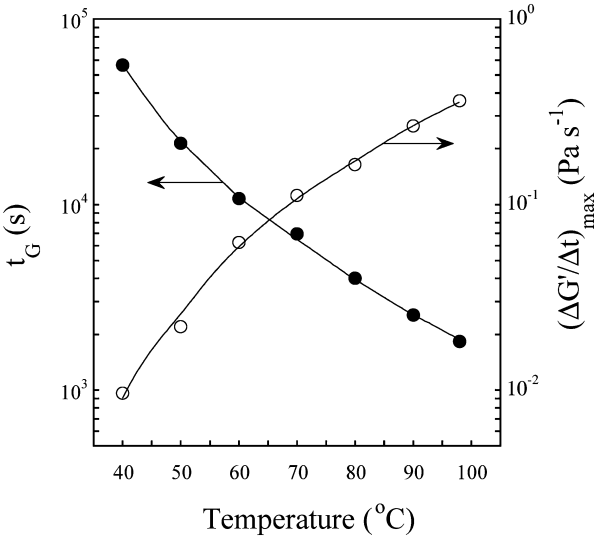

Fig. 3 The gelation time, t_G (●), and the maximum gelation rate, $(\Delta G'/\Delta t)_{max}$ (○), of a 1.5 wt% chitosan–25 mM DHF solution as a function of temperature. The pH was 1.4. In all cases, t_G was calculated using the G'-G" crossover method of Tung and Dynes [78]

chitosan–DHF gelation are more quantitatively assessed in Fig. 3, where both the gelation time, t_G (equated with the time at which G' = G", such that $\delta = 45°$)[1] and the maximum rate of G' increase with time, $(\Delta G'/\Delta t)_{max}$, are shown. A systematic decrease in t_G, and increase in $(\Delta G'/\Delta t)_{max}$ with rising temperature are clearly evident, indicating a substantial increase in the rate of gelation as a function of rising temperature.

A more detailed examination of the rheological behaviour observed in Figs. 1 and 2 warrants consideration of the underlying gelation mechanism. Chitosan–DHF gelation is the product of a two-step reaction process. In the first step, DHF reacts with protons in acidic solution and decomposes to form butenedial according to Scheme 1 [72].

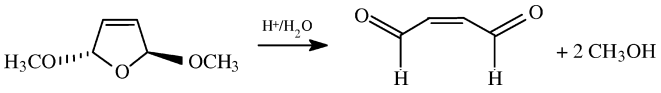

Scheme 1

In a second reaction step (Scheme 2), the carbonyl groups of butenedial then react with the amine moieties of chitosan to form covalent inter-molecular links between adjacent chitosan molecules:

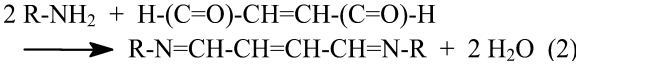

Scheme 2

where R represents the non-reacting remainder of each chitosan molecule.

The relative impacts of the two reaction steps on the overall reaction rate can be assessed with reference to both the t_G data of Fig. 3 and previous investigations into the gelation of chitosan by glutaraldehyde, H–(C=O)$(CH_2)_3$(C=O)–H, a dialdehyde crosslinker comparable to butenedial. For the lowest temperature chitosan–DHF system examined in this study (40 °C), t_G is found to occur at 56 500 s (15.7 h). By comparison, Mi et al. [33] have recently examined the gelation kinetics of the same high molecular weight (MW = 2 000 000) chitosan by glutaraldehyde over a range of moderate temperatures (18–30 °C). They found that even at a slightly lower chitosan concentration (1 wt%, compared with 1.5 wt% in this study), crosslinker concentration (0.25 wt%, compared with 0.33 wt% in Figs. 1, 2 and 3), and temperature (30 °C, compared with the 40 °C chitosan–DHF system considered here), t_G occurred after only 175 s; that is, on a time scale 320 times faster than observed for the analogous chitosan–DHF system in the present study. Such findings strongly suggest that the reaction between chitosan and butenedial should be similarly rapid, and indicate that of the two reaction steps underlying gelation of chitosan by DHF, it is the first (i.e. decomposition of DHF to form butenedial) that is rate-determining. As is suggested by an examination of the stoichiometry of Scheme 1 and indicated by the exponential form of the DHF concentration versus time data of Hansen et al. [72], this rate-determining step is first-order with respect to DHF.

Interestingly, the t_G data shown in Fig. 3 can also be used to define a common stage of reaction at which an Arrhenius-type treatment can be performed (e.g. [79, 80]), allowing calculation of the apparent activation energy using the relationships:

[1] The strict definition of t_G has been considered in detail by Chambon and Winter [75, 76, 77], who defined it as the condition at which tan(G"/G') is independent of frequency. Their treatment requires accurate measurements of G' and G" over a wide range of frequencies both before and after t_G and additionally, requires that G' and G" do not vary appreciably during each frequency sweep. Unfortunately, in the present study, G' and G" were difficult to accurately assess prior to t_G due to measurements being undertaken at the lower stress limit of the rheometer. In addition, during the gelation process, G' and G" were often found to vary significantly over the duration of each frequency sweep. As a result, t_G could not be accurately assessed using the treatment of Chambon and Winter [75, 76, 77]. The G'-G" crossover method of Tung and Dynes [78] was instead used and, while not providing a strict measure of t_G, does allow a comparison of the crosslinking behaviour at a common stage of gelation. It is, however, worthy of note that given the change in δ from ca. 80° to $\leq 1°$ is rapid, particularly at the higher temperatures investigated (see Fig. 2), it is expected that the values of t_G calculated using the G'-G" crossover method are in reasonable agreement with the Chambon and Winter gel point definition.

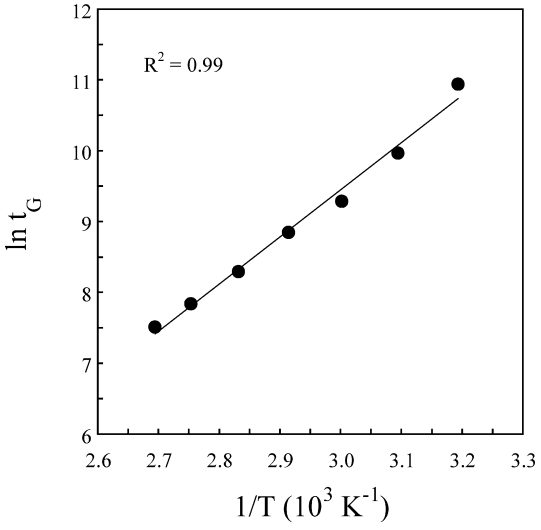

Fig. 4 Arrhenius plot of ln t_G versus 1/T for a 1.5 wt% chitosan–25 mM DHF solution. The pH was 1.4

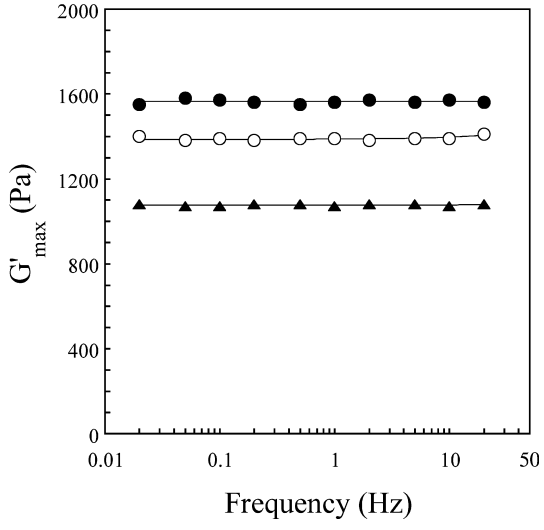

Fig. 5 The maximum storage modulus, G'_{max}, measured for a 1.5 wt% chitosan–25 mM DHF solution as a function of temperature and frequency. ● 60 °C, ○ 80 °C, ▲ 98 °C

$$k = A \exp\left(\frac{-E_a}{RT}\right) \quad (1)$$

and

$$t_G = \frac{c}{k} \quad (2)$$

such that

$$\ln t_G = \frac{E_a}{RT} + C \quad (3)$$

where k is the rate constant, A is the so-called kinetic pre-exponential factor (a constant), R is the gas constant, and both c and C are constants.

The resulting plot of ln t_G versus 1/T (Fig. 4) yields an apparent activation energy, E_a, of 55 ± 8 kJ mol^{-1}. The calculated value of E_a is understandably higher than that determined by Mi et al. [33] for the gelation of a high molecular weight chitosan by glutaraldehyde ($E_a = 49.6$ kJ mol^{-1}), but is substantially lower than that calculated by Hansen et al. [72] for the reaction of DHF with polyvinyl alcohol (PVA) ($E_a \geq 74$ kJ mol^{-1}). A number of explanations are possible for this lower E_a value, including differences in the reactivity of dialdehyde molecules with polymeric amine and alcohol moieties, and experimental differences in the polymer molecular weights. Mi et al. [33] have recently reported that the latter parameter significantly affects the E_a value calculated for the reaction of chitosan with glutaraldehyde.

Interestingly, in addition to the gelation characteristics discussed above, Fig. 1 also shows that at all but the lowest temperatures studied, the chitosan–DHF gels reach an upper strength limit (as defined by the maximum in G', G'_{max}), beyond which G' decreases. The limiting gel strength is greatest at 60–70 °C, is frequency-independent (typical of elastic gel formation in polysaccharide solutions: see Fig. 5) and diminishes significantly at higher temperatures. Two possible explanations for this behaviour exist, namely syneresis (a process whereby a gelled body contracts in size upon reaching a critical network pressure, expelling free water) and thermal decomposition of the gelled body. Syneresis was eliminated from consideration by direct measurements of free water expelled from the gel body, which showed that for a selected system (80 °C), no syneresis occurred in the vicinity of the time at which the decrease in G' commenced, and only a very small extent of syneresis (4%) occurred over the duration of the experiment. Instead, we believe that the reduction in G' at times beyond the occurrence of G'_{max} can be rationalized with reference to chitosan depolymerization phenomena, as are discussed in the following section.

Impact of temperature on degradation of chitosan–DHF gels

A number of previous studies have demonstrated that when solubilized in aqueous HCl environments, chitosan will gradually decompose via hydrolysis of the glycosidic linkages to yield glucosamine oligosaccharides (e.g. [81, 82]). From a rheological perspective, the depolymerization process is expected to significantly reduce the extent of inter-chain entanglements. A decrease in the measured shear viscosity, η_s, should then result. This behaviour is demonstrated in Fig. 6, where η_s is shown as a function of both shear rate and time of thermal exposure at 80 °C. The solution pH is again 1.4. Prior to

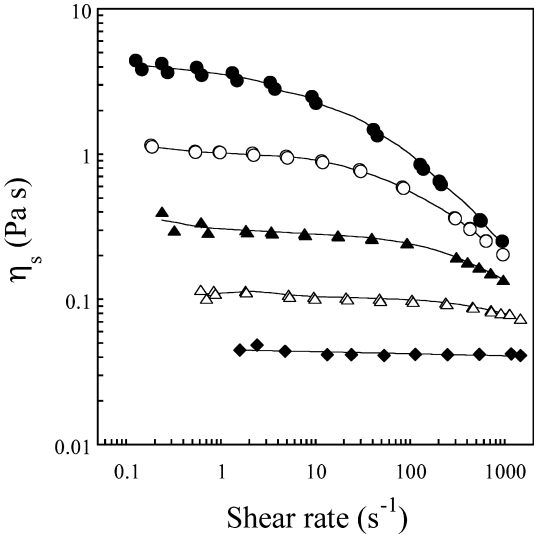

Fig. 6 The shear viscosity, η_s, versus shear rate properties of a 1.5 wt% chitosan solution at pH 1.4 after heating at 80 °C for various periods of time. All measurements of η_s were conducted at a temperature of 20 °C. The time of heating was ● 0 s, ○ 1 500 s, ▲ 5 000 s, △ 11 000 s, ◆ 20 000 s

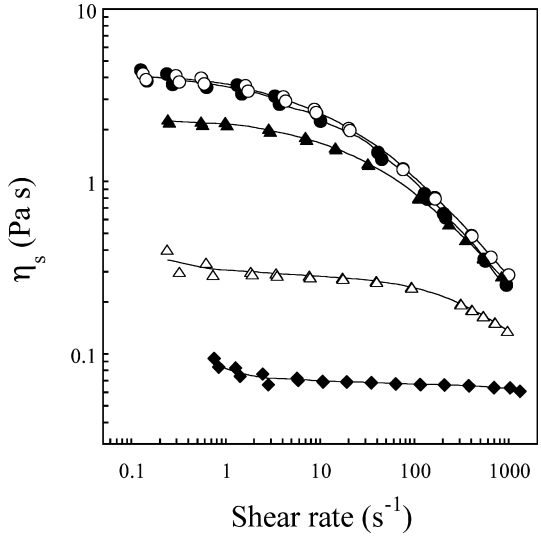

Fig. 7 The shear viscosity versus shear rate properties of a 1.5 wt% chitosan solution at pH 1.4 after heating at various temperatures for a time period of 5 000 s. All measurements of η_s were conducted at a temperature of 20 °C. The temperature of heat treatment was ● 20 °C, ○ 40 °C, ▲ 60 °C, △ 80 °C, ◆ 95 °C

heating at 80 °C, Fig. 6 shows that the chitosan solution is strongly shear thinning in nature, consistent with a systematic alignment of the high molecular weight chitosan chains with the shear field as the shear rate increases [83, 84, 85]. When heated at 80 °C, Fig. 6 shows that the shear viscosity decreases significantly, and η_s gradually becomes less sensitive to the shear rate. At the longest exposure time examined (20 000 s), Fig. 6 also shows that the flow behaviour is almost Newtonian in nature. Such findings are consistent with a systematic decrease in the molecular weight of the chitosan chains, resulting in a gradual elimination of inter-chain entanglements and an associated decrease in the shear sensitivity of the molecular alignment [85].

In addition to its time dependence, the rate of chitosan decomposition is strongly dependent upon the solution temperature. For example, Fig. 7 shows that after 5 000 s, exposure of a chitosan solution at pH 1.4 to a temperature of 40 °C does not lead to a significant change from its initial shear viscosity behaviour. However, at temperatures in excess of 40 °C over the same period of time, Fig. 7 shows that η_s decreases as a function of increasing temperature and becomes systematically less sensitive to shear rate. The latter findings indicate that the rate of depolymerization rises markedly as the solution temperature is increased.

The data of Figs. 6 and 7 indicate that the chitosan–DHF crosslinking process should be viewed as one in which the interconnectivity of the gelled body is promoted by the reaction with DHF (increasing the network strength) and disrupted by acid depolymerization of chitosan (decreasing the network strength). It therefore follows that the limiting G' value measured at each temperature corresponds to the maximum degree of interconnectivity, and is largely determined by the relative rates of the crosslinking and depolymerization processes. The data of Fig. 1 suggest that despite promoting a greater initial rate of DHF conversion into butenedial (leading to an increased initial rate of gelation), the increased rate of depolymerisation induced by the application of high temperatures is sufficient to generate smaller limiting network strengths (i.e. lower limiting degrees of interconnectivity) than are obtained at lower temperatures. As a result, G'_{max} decreases as a function of increasing temperature, and the rate of decrease of G' at times beyond the measurement of G'_{max} is greatest at the highest temperatures examined.

It should be noted that the occurrence of acid-promoted chitosan depolymerization is not expected to have impacted significantly on the value of E_a calculated for the chitosan–DHF gelation process. Experimentally, this is due to the substantially higher initial rate of the chitosan–DHF crosslinking reaction versus the initial rate of depolymerization, as evidenced by the substantial increases in G' and decreases in δ (indicative of an initial rapid rise in the degree of network interconnectivity). From a theoretical standpoint, the markedly lower activation energy of the chitosan–DHF crosslinking reaction ($E_a = 55$ kJ mol^{-1}) versus that of the depolymerization process ($E_a = 130$–160 kJ mol^{-1} [82]) provides additional evidence that the initial reaction process will be dominated by the crosslinking reaction. Even considering the lower E_a value (130 kJ mol^{-1} [82]) for the depolymerization process, such differences in activation energy will

cause the exponential component of Eq. 1 to be 10^{10} to 10^{12} times larger for the crosslinking versus the depolymerization reaction over the range of temperatures investigated here. In combination with the similar initial concentrations of the reactants for the crosslinking ([DHF] = 25 mM, $[H^+]$ = 40 mM) and depolymerization ([chitosan glycosidic linkages]≈90 mM, $[H^+]$ = 40 mM) processes, such extreme differences in the values of the exponential component of Eq. 1 (and therefore in the rate constant, k) strongly suggest that the chitosan–DHF crosslinking reaction will be initially dominant. The effects of chitosan depolymerization will then become increasingly important as DHF is consumed, and the rate of the crosslinking reaction slows.

Impact of DHF concentration on chitosan–DHF gelation kinetics

An increase in the concentration of DHF in solution is expected to lead to a corresponding rise in the rate of butenedial formation from DHF (see Scheme 1), and therefore an increase in both the rate and extent of gel formation. This effect is demonstrated in Fig. 8, where G' is presented as a function of time and DHF concentration for a 1.5 wt% chitosan solution. The pH is 1.4 and the temperature is 80 °C. Figure 8 shows that the limiting gel strength (as given by G'_{max}) rises markedly as the DHF concentration increases. In addition, Fig. 8 shows that over the range of DHF concentrations examined, $\Delta G'/\Delta t$ initially increases as the DHF concentration rises. This behaviour is supported by the corresponding phase lag properties (Fig. 9), which generally show that $\delta \rightarrow 0$ most rapidly at the highest DHF concentrations investigated. Interestingly, Fig. 9 also shows that at the lowest DHF concentration examined ([DHF] = 10 mM), δ reaches a limiting lower value of only 15°. In combination with the low magnitude of G'_{max} measured for this system (ca. 20 Pa), this relatively high value of δ indicates that insufficient crosslinking agent exists at [DHF] = 10 mM to allow strong gel formation to occur.

A substantial enhancement of the rate of chitosan–DHF gelation with increasing DHF concentration is also indicated by Fig. 10, in which the gelation time,

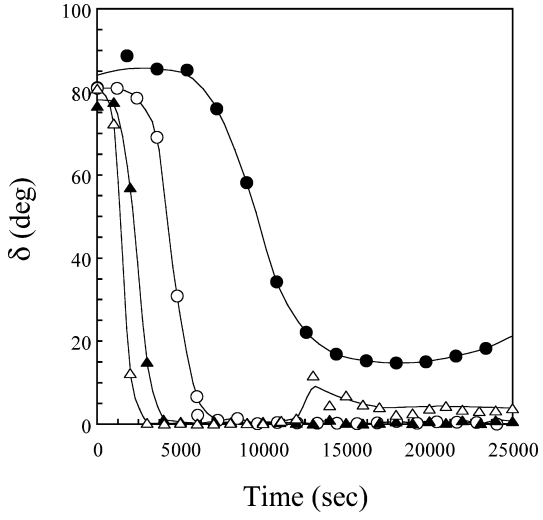

Fig. 9 The phase lag, δ, measured for a 1.5 wt% chitosan solution at pH 1.4 as a function of both DHF concentration and time. The temperature was 80 °C. The DHF concentration was ● 10 mM, ○ 25 mM, ▲ 50 mM, △ 100 mM

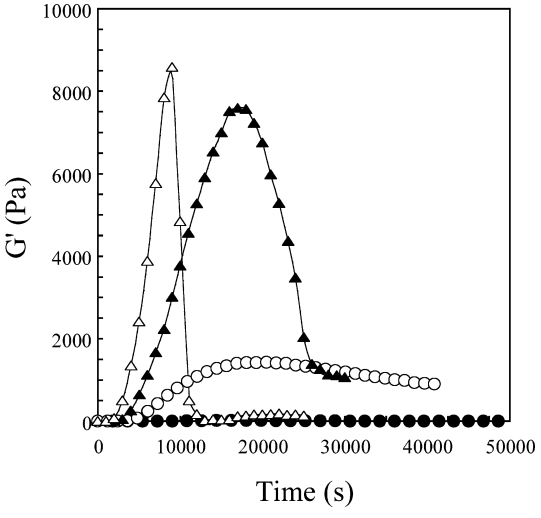

Fig. 8 The storage modulus of a 1.5 wt% chitosan solution at pH 1.4 as a function of both DHF concentration and time. The temperature was 80 °C. The DHF concentration was ● 10 mM, ○ 25 mM, ▲ 50 mM, △ 100 mM

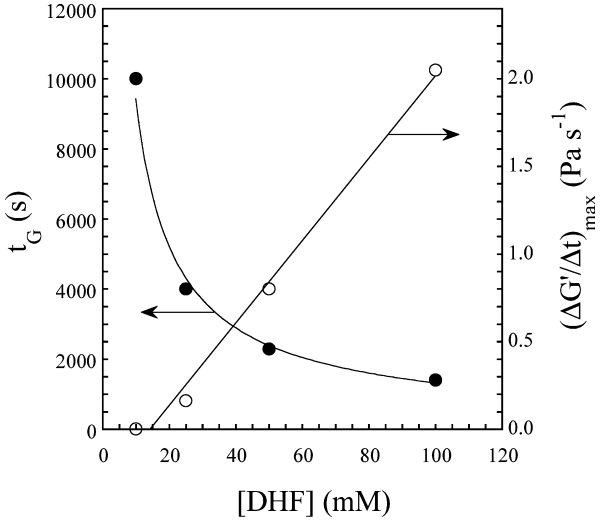

Fig. 10 The gelation time, t_G (●), and the maximum gelation rate, $(\Delta G'/\Delta t)_{max}$ (○), of a 1.5 wt% chitosan solution as a function of DHF concentration at 80 °C. The pH was 1.4

t_G, and maximum rate of increase of G' with time, $(\Delta G'/\Delta t)_{max}$, are shown. Over the range of DHF concentrations investigated, t_G is inversely correlated with DHF concentration ($r^2 = 1.00$), and as a result, rises dramatically as [DHF] is reduced. By contrast, $(\Delta G'/\Delta t)_{max}$ is closely correlated with [DHF] ($r^2 = 0.99$), and therefore increases substantially as a function of increasing DHF concentration. The intercept of the $(\Delta G'/\Delta t)_{max}$ versus [DHF] data at 0 Pa s^{-1} occurs in the vicinity of the 10 mM data point, and is taken to approximately represent the minimum crosslinker concentration required to allow gelation to occur.

Interestingly, Fig. 8 also shows that the time at which G'_{max} is measured decreases as the DHF concentration increases. In addition, the rate at which G' decreases at times beyond the measurement of G'_{max} is greatest at the highest DHF concentrations. These properties cannot be explained with reference to chitosan depolymerization processes given that the chitosan–DHF crosslinking reaction would have continued to dominate the chitosan depolymerization process for the longest times in solutions containing the highest DHF concentrations. Instead, the G' versus time behaviour obtained subsequent to the measurement of G'_{max} can be rationalized with reference to the syneresis properties of the crosslinked gels.

Characteristically observed in strong polysaccharide gels including some crosslinked chitosan systems (e.g. [20, 86]), syneresis is a process that occurs when the crosslink density reaches a critical point at which the network pressure exceeds the osmotic counter-pressure generated by water bound within the gel structure. As a result, the gelled body contracts in size, expelling free water. When occurring during cone-and-plate oscillatory rheometry, syneresis can affect experimental measurements by causing the gel to shrink away from the cone. The contact area between the gel and the cone is therefore reduced, leading to the measurement of an apparent decrease in the gel strength.

Table 1 shows the extent of syneresis (defined as the percentage of the total gel mass expelled as free water) measured at 80 °C for 1.5 wt% chitosan solutions as a function of DHF concentration and time. The pH is again 1.4. For the lowest DHF concentration examined ([DHF] = 25 mM), Table 1 shows that syneresis occurs only after ca. 30 000 s, well beyond the time at which G'_{max} is measured (see Fig. 8). Even at this long thermal exposure time, the extent of syneresis is low. Syneresis occurs more rapidly at to a greater extent at a DHF concentration of 50 mM, with its onset being in approximate agreement with the time at which G'_{max} is measured. In this case, therefore, slight shrinkage of the gel away from the rheometer cone is likely to be at least partially responsible for the more rapid reduction in G' beyond G'_{max}. At a DHF concentration of 100 mM, far more rapid and extensive syneresis behaviour is observed. For example, Table 1 shows that over 30% of the total gel mass has been expelled as free water after only 5 000 s of exposure at 80 °C, and nearly 60% has been released after 10 000 s. Such behaviour will lead to a large reduction in the contact area between the gel and the rheometer cone, and makes it unsurprising that G' reaches a limiting value over a relative short time-frame, beyond which is rapidly decreases. Gel shrinkage (and the consequential formation of a layer of chitosan-depleted solution in contact with some regions of the cone) is also consistent with the increase in δ measured at [DHF] = 100 mM and times in excess of 13 000 s in Fig. 9.

Table 1 The syneresis properties of a 1.5 wt% chitosan solution at pH 1.4 as a function of both DHF concentration and time of thermal exposure at 80 °C. The extent of syneresis is defined as the percentage of the total gel mass expelled as free water

Time	Extent of syneresis (%)		
(s)	[DHF] = 25 mM	[DHF] = 50 mM	[DHF] = 100 mM
2 000	0	0	0
5 000	0	0	34
10 000	0	0	59
20 000	0	10	71
30 000	4	16	79

Impact of pH on chitosan–DHF gelation kinetics

The solution pH is expected to affect the rate and extent of chitosan gelation by determining the rates at which both the conversion of DHF into butenedial (see Scheme 1) and the depolymerization of chitosan occur. Hansen et al. [72] have demonstrated that at a given temperature, the rate of butenedial formation from DHF rises as pH decreases. Similarly, the rate of depolymerization of chitosan increases as a function of decreasing pH, as indicated by the shear viscosity, η_s, data presented in Fig. 11 for a 1.5 wt% chitosan solution after exposure at 80 °C for 5 000 s. Here, the decrease in η_s becomes systematically greater, and the approach to Newtonian flow behaviour more pronounced, as the pH is lowered, indicating a higher degree of depolymerization at the lowest pH values examined. The overall rate and extent of chitosan–DHF gelation at a given pH condition is therefore expected to be governed by the respective rates at which butenedial formation and chitosan depolymerization occur.

Figure 12 shows the G' properties measured for a 1.5 wt% chitosan–25 mM DHF solution at 80 °C as a function of both time and pH. Over the range of low pH conditions examined (pH ≤ 2.1), Fig. 12 shows that the initial rate of increase of G', $\Delta G'/\Delta t$, increases markedly as a function of decreasing pH. Similarly, the corre-

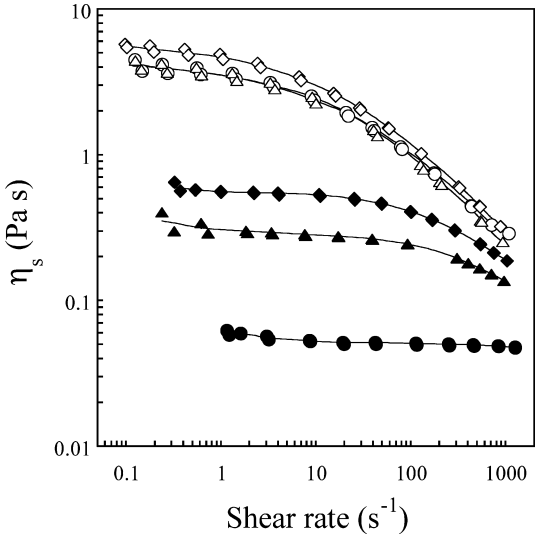

Fig. 11 The shear viscosity versus shear rate properties of a 1.5 wt% chitosan solution as a function of pH both before (*open symbols*) and after (*filled symbols*) heating for 5 000 s at 80 °C. All measurements of η_s were conducted at a temperature of 20 °C. The pH was ○,● 0.9; △,▲ 1.4; ◇,◆ 3.1

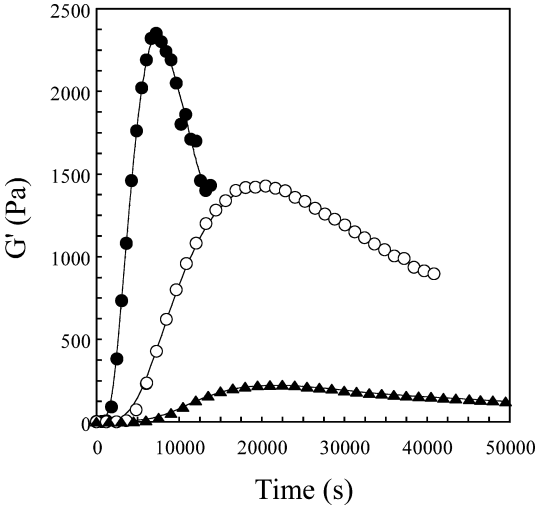

Fig. 12 The storage modulus of a 1.5 wt% chitosan–25 mM DHF solution as a function of both time and pH. The temperature was 80 °C. The pH was ● 0.9, ○ 1.4, ▲ 2.1

sponding phase lag versus time data, presented in Fig. 13, show that $\delta \rightarrow 0$ most rapidly at the lowest pH values investigated. These findings indicate that the initial rate of chitosan–DHF gelation increases as a function of decreasing pH. Figure 12 also shows that G'_{max} is of greatest magnitude, and occurs on the smallest experimental time-frame, at the most acidic pH conditions investigated. The rate of decrease of G' at times beyond the measurement of G'_{max} is similarly greatest at the lowest pH conditions examined.

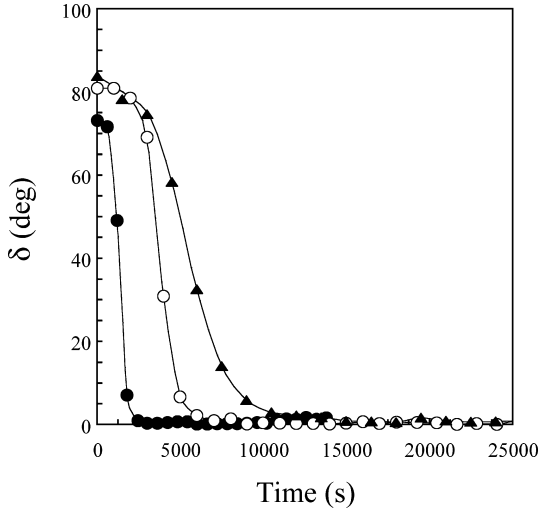

Fig. 13 The phase lag, δ, measured for a 1.5 wt% chitosan–25 mM DHF solution as a function of both time and pH. The temperature was 80 °C. The pH was ● 0.9, ○ 1.4, ▲ 2.1

The above findings suggest that the rate of DHF conversion into butenedial (and therefore the rate of chitosan–DHF gelation) initially increases to a substantially greater extent than does the rate of chitosan depolymerization as a function of decreasing pH. Higher initial values of $\Delta G'/\Delta t$ result, and lead to G'_{max} being greatest at the most acidic conditions examined. As the concentration of DHF is depleted, however, the rate of crosslinking will slow. The chitosan depolymerization process is therefore expected to become increasingly significant as time progresses, and eventually, at a time given by that at which G'_{max} is measured, will surpass the rate of the crosslinking reaction. The more rapid rate of DHF depletion coupled with a higher rate of chitosan depolymerization causes G'_{max} to occur on a smaller time-frame at the most acidic pH conditions investigated. Presumably, as no significant syneresis was observed for these systems, the higher rate of chitosan depolymerization is also responsible for the more rapid decrease in G' measured at times beyond G'_{max} for the lowest pH systems examined.

In addition to the results presented at pH ≤ 2.1 in Figs. 12 and 13, we performed several additional series of rheological measurements at higher pH values (not shown). In those cases, however, the results were complicated by substantial rises in pH that occurred as protons were consumed during the conversion of DHF to butenedial (see Scheme 1). A rapid and substantial change in the solubility of chitosan resulted (as has previously been reported as the solution pH approaches the pK_a of the chitosan amine moieties, e.g. [87, 88]), leading to the rapid formation of relatively weak gel networks. By contrast, reductions in chitosan solubility

were not found to significantly affect the results shown in Figs. 12 and 13 due to the markedly lower initial pH conditions utilized, which protected against substantial rises in pH during the initial gelation process.

Conclusions

The gelation of an aqueous chitosan–2,5-dimethoxy-2,5-dihydrofuran (DHF) system has been rheologically examined as a function of temperature, DHF concentration and pH. The findings can be summarized as follows:

1. The gelation time, t_G, decreases, and the initial rate of gelation increases as a function of rising temperature. The G' versus time behaviour indicates that the mechanical strength of the gel initially increases before passing through a maximum value and then diminishing. The magnitude of G'_{max} is lowest at the highest temperatures examined. Each of these findings can be justified in terms of the competition between the chitosan–DHF crosslinking reaction (which dominates initially) and protolytic depolymerization of chitosan (which becomes increasingly important as time progresses). The apparent activation energy for the gelation process is 55 ± 8 kJ mol^{-1}.
2. The rate of gelation and magnitude of G'_{max} increase as a function of rising DHF concentration. Such results are consistent with an increase in the rate of DHF conversion into butenedial (a process which is first-order with respect to DHF), leading to a corresponding increase in the rate and extent of gelation. Syneresis phenomena are found to lead to a dramatic decrease in G' at times beyond the measurement of G'_{max} for DHF concentrations ≥50 mM.
3. At pH ≤ 2.1, both the rate of gelation and the magnitude of G'_{max} increase as a function of decreasing pH. In addition, the time at which G'_{max} is measured is lower for the more acidic chitosan–DHF systems. These findings are again consistent with a competition between chitosan–DHF crosslinking (which is initially dominant) and protolytic depolymerization of chitosan.

The combined results allow us to define appropriate reaction conditions for the chitosan–DHF system for cases in which controlled crosslinking to yield strong, rigid gels is desired while avoiding significant complications from syneresis phenomena. These conditions are: temperature 60–80 °C, [DHF]≈25 mM, and pH≈1.

Acknowledgements Financial support for this work provided through the Australian Research Council's Small Grants program.

References

1. Mathur NK, Narang CK (1990) J Chem Edu 67:938–942
2. Sandford PA, Hutchings GP (1987) Chitosan—a natural, cationic biopolymer: commercial applications. In: Yalpani M (ed) Industrial polysaccharides: genetic engineering, structure/property relations and applications. Elsevier, Amsterdam
3. Chirkov SN (2002) Appl Biochem Microbiol 38:1-8
4. Tharanathan RN, Kittur FS (2003) Crit Rev Food Sci Nutrition 43:61–87
5. Shahidi F, Arachchi JKV, Jeon YJ (1999) Trends Food Sci Technol 10:37–51
6. Kumar MNVR (2000) React Funct Polym 46:1-27
7. Dutta PK, Ravikumar MN, Dutta J (2002) J Macromol Sci Polym Rev C42:307–354
8. Singh DK, Ray AR (2000) J Macromol Sci Rev Macromol Chem Phys C40:69–83
9. Peter MG (1995) J Macromol Sci Pure Appl Chem A32:629–640
10. Borchard G (2001) Adv Drug Deliv Rev 52:145–150
11. Ueno H, Mori T, Fujinaga T (2001) Adv Drug Deliv Rev 52:105–115
12. Paul W, Sharma CP (2000) STP Pharma Sci 10:5-22
13. Struszczyk MH (2002) Polimery 47:396–403
14. Rathke TD, Hudson SM (1994) J Macromol Sci Rev Macromol Chem Phys C34:375–437
15. Dodane V, Vilivalam VD (1998) Pharm Sci Technol Today 1:246–253
16. Amiji MM (1995) Carbohydrate Polym 26:211–213
17. Ottoy MH, Varum KM, Christensen BE, Anthonsen MW, Smidsrod O (1996) Carbohydrate Polym 31:253–261
18. Schatz C, Viton C, Delair T, Pichot C, Domard A (2003) Biomacromol 4:641–648
19. Arguelles-Monal W, Goycoolea FM, Peniche C, Higuera-Ciapara I (1998) Polym Gels Networks 6:429–440
20. Roberts GAF, Taylor KE (1989) Makromol Chem 190:951–960
21. Knaul JZ, Hudson SM, Creber KAM (1999) J Polym Sci B—Polym Phys 37:1079–1094
22. Wei YC, Hudson SM, Mayer JM, Kaplan DL (1992) J Polym Sci A—Polym Chem 30:2187–2193
23. Thacharodi D, Rao KP (1993) J Chem Technol Biotechnol 58:177–181
24. Mi FL, Shyu SS, Lee ST, Wong TB (1999) J Polym Sci B—Polym Phys 37:1551–1564
25. Matsuyama H, Kitamura Y, Naramura Y (1999) J Appl Polym Sci 72:397–404
26. Nakatsuka S, Andrady AL (1992) J Appl Polym Sci 44:17–28
27. Thacharodi D, Rao KP (1993) Int J Pharm 96:33–39
28. Thanoo BC, Sunny MC, Jayakrishnan A (1992) J Pharm Pharmacol 44:283–286
29. Jameela SR, Kumary TV, Lal AV, Jayakrishnan A (1998) J Controlled Release 52:17–24
30. Nigalaye AG, Adusumilli P, Bolton S (1990) Drug Dev Ind Pharm 16:449–467

31. Kawashima Y, Handa T, Kasai A, Takenaka H, Lin SY, Ando Y (1985) J Pharm Sci 74:264–268
32. Hsien TY, Rorrer GL (1995) Sep Sci Technol 30:2455–2475
33. Mi FL, Kuan CY, Shyu SS, Lee ST, Chang SF (2000) Carbohydrate Polym 41:389–396
34. Hou WM, Miyazaki S, Takada M, Komai T (1985) Chem Pharm Bull 33:3986–3992
35. Jameela SR, Latha PG, Subramoniam A, Jayakrishnan A (1996) J Pharm Pharmacol 48:685–688
36. Filipovic-Grcic J, Becirevic-Lacan M, Skalko N, Jalsenjak I (1996) Int J Pharm 135:183–190
37. Nishioka Y, Kyotani S, Okamura M, Miyazaki M, Okazaki K, Ohnishi S, Yamamoto Y, Ito K (1990) Chem Pharm Bull 38:2871–2873
38. Ko JA, Park HJ, Hwang SJ, Park JB, Lee JS (2002) Int J Pharm 249:165–174
39. Hassan EE, Parish RC, Gallo JM (1992) Pharm Res 9:390–397
40. Shiraishi S, Imai T, Otagiri M (1993) J Controlled Release 25:217–225
41. Akbuga J, Durmaz G (1994) Int J Pharm 111:217–222
42. Jameela SR, Misra A, Jayakrishnan A (1994) J Biomat Sci Polym Ed 6:621–632
43. Ohya Y, Shiratani M, Kobayashi H, Ouchi T (1994) J Macromol Sci Pure Appl Chem A31:629–642
44. Wan LSC, Lim LY, Soh BL (1994) STP Pharma Sci 4:195–200
45. Sezer AD, Akbuga J (1995) Int J Pharm 121:113–116
46. Aydin Z, Akbuga J (1996) Int J Pharm 131:101–103
47. Berthold A, Cremer K, Kreuter J (1996) J Controlled Release 39:17–25
48. Kas HS (1997) J Microencapsulation 14:689–711
49. Al Helw AA, Al Angary AA, Mahrous GM, Al Dardari MM (1998) J Microencapsulation 15:373–382
50. Gupta KC, Kumar MNVR (1999) J Macromol Sci Pure Appl Chem A36:827–841
51. Koseva N, Stoilova O, Manolova N, Rashkov I, Madec PJ (2001) J Bioactive Compat Polym 16:3-19
52. Kumbar SG, Kulkarni AR, Aminabhavi TM (2002) J Microencapsulation 19:173–180
53. Dini E, Alexandridou S, Kiparissides C (2003) J Microencapsulation 20:375–385
54. Kawase M, Michibayashi N, Nakashima Y, Kurikawa N, Yagi K, Mizoguchi T (1997) Biol Pharm Bull 20:708–710
55. Senkoylu A, Simsek A, Sahin FI, Menevse S, Ozogul C, Denkbas EB, Piskin E (2001) J Bioactive Compat Polym 16:136–144
56. Zeng X, Ruckenstein E (1998) J Membrane Sci 148:195–205
57. Zeng X, Ruckenstein E (1998) Ind Eng Chem Res 37:159–165
58. Vincent T, Guibal E (2002) Ind Eng Chem Res 41:5158–5164
59. Kurita K (1987) Binding of metal cations by chitin derivatives: improvement of adsorption ability through chemical modifications. In: Yalpani M (ed) Industrial polysaccharides: genetic engineering, structure/property relations and applications. Elsevier, Amsterdam
60. Ohga K, Kurauchi Y, Yanase H (1987) Bull Chem Soc Jpn 60:444–446
61. Hsien TY, Rorrer GL (1997) Ind Eng Chem Res 36:3631–3638
62. Kawamura Y, Yoshida H, Asai S, Kurahashi I, Tanibe H (1997) Sep Sci Technol 32:1959–1974
63. Guibal E, Milot C, Roussy J (1999) Wat Environ Res 71:10–17
64. Ruiz M, Sastre AM, Zikan MC, Guibal E (2001) J Appl Polym Sci 81:153–165
65. Yang Z, Zhuang L, Tan G (2002) J Appl Polym Sci 85:530–535
66. Juang RS, Shao HJ (2002) Adsorption 8:71–78
67. Chiou MS, Li HY (2002) J Hazard Mat 93:233–248
68. Oshita K, Oshima M, Gao YH, Lee KH, Motomizu S (2002) Anal Sci 18:1121–1125
69. Ngah WSW, Endud CS, Mayanar R (2002) React Funct Polym 50:181–190
70. Jaworska M, Kula K, Chassary P, Guibal E (2003) Polym Int 52:206–212
71. Chiou MS, Li HY (2003) Chemosphere 50:1095–1105
72. Hansen EW, Holm KH, Jahr DM, Olafsen K, Stori A (1997) Polymer 38:4863–4871
73. Johnson SB, Dunstan DE, Franks GV (2002) J Am Ceram Soc 85:1699–1705
74. Merkovich EA, Carruette ML, Babak VG, Vikhoreva GA, Gal'braikh LS, Kim VE (2001) Colloid J 63:350–354
75. Chambon F, Winter HH (1985) Polym Bull 13:499–503
76. Winter HH, Chambon F (1986) J Rheol 30:367–382
77. Chambon F, Winter HH (1987) J Rheol 31:683–697
78. Tung CYM, Dynes PJ (1982) J Appl Polym Sci 27:569–574
79. Nolte H, John S, Smidsrod O, Stokke BT (1992) Carbohydrate Polym 18:243–251
80. Park SJ, Kim TJ, Lee JR (2000) J Polym Sci B—Polym Phys 38:2114–2123
81. Domard A, Cartier N (1989) Int J Biol Macromol 11:297–302
82. Varum KM, Ottoy MH, Smidsrod O (2001) Carbohydrate Polym 46:89–98
83. Mucha M (1997) Macromol Chem Phys 198:471–484
84. Kienzle-Sterzer CA, Rodriguez-Sanchez D, Rha CK (1985) Polym Bull 13:1-6
85. Lapasin R, Pricl S (1995) Rheology of industrial polysaccharides: theory and applications. Blackie Academic, London
86. Moore GK, Roberts GAF (1980) Int J Biol Macromol 2:73–77
87. Claesson PM, Ninham BW (1992) Langmuir 8:1406–1412
88. Varum KM, Ottoy MH, Smidsrod O (1994) Carbohydrate Polym 25:65–70